JOURNAL OF MATERIALS SCIENCE 31 (1996) 6627–6630

Thermal oxidation-resistant surface alloys processed by laser alloying on 35 NCD 16 ferritic steel

E. GEMELLI, A. GALERIE, M. CAILLET
Laboratoire Science des Surfaces et Matériaux Carbonés, URA CNRS 413, Ecole Nationale Supérieure d'Electrochimie et d'Electrométallurgie de Grenoble, Institut National Polytechnique de Grenoble, BP 75 Domaine Universitaire, 38402 Saint-Martin d'Hères, France

The hardness and the high-temperature oxidation resistance of the low-alloyed ferritic steel 35 NCD 16 (Fe–0.38 C–1.8 Cr–4 Ni, wt%) were increased by laser surface alloying of Cr_3C_2 or Cr_3C_2 and SiC. The obtained surface alloys always exhibit primary dendrites (γ Fe solid solution with Cr and Si + martensite) and an interdendritic eutectic containing γ Fe + martensite + M_7C_3 carbides (M = Fe, Cr). In the first case, the formation of iron chromite, $FeCr_2O_4$, in contact with the coating accounts for the good oxidation resistance. In the second case, the beneficial influence of silicon lies in the formation in the presence of oxygen of a thin chromia scale only, with local silicon enrichment, showing excellent barrier properties. Kinetic and structural observations are discussed in the light of thermodynamics and diffusion processes.

1. Introduction

The use of lasers in surface engineering affords interesting properties to materials exposed to aggressive environments [1–3]. Such a surface treatment can improve mechanical and/or chemical properties, particularly if alloying with foreign species takes place. For example, the thermal oxidation of steels is reduced by chromium or silicon additions, easily achieved superficially by laser alloying. The mode of action of these two elements is similar, leading to the growth, during oxidation, of mixed oxides such as $FeCr_2O_4$ or $FeSi_2O_4$ for low amounts and of only Cr_2O_3 or SiO_2 for higher amounts. The difference lies in the minimum concentration needed for the growth of the simple oxides: 13 wt% for chromium [4–8] and only 3 wt% for silicon [9, 10]. Such oxides are very efficient barriers to metal and oxygen transport, and constitute highly protective layers.

The simultaneous use of both chromium and silicon in steels has also been envisaged [11, 12]. Silicon oxide can then form between the steel and a chromium-containing oxide layer. The minimum concentration in the steel to form a continuous SiO_2 layer during oxidation decreases as the chromium concentration in the steel increases. In addition, the presence of silicon reduces the chromium concentration to allow the growth of a pure Cr_2O_3 oxide layer. For example, additions of 1–2 wt% Si to Fe–9 Cr or Fe–8 Cr–10 Ni alloys is enough to allow the growth of a continuous Cr_2O_3 layer [13].

As carbon addition is well known to improve steel hardness by solute and/or precipitation effects, we chose to investigate chromium carbide and silicon carbide additions to improve both high-temperature oxidation and wear resistance of a low-alloyed steel. Another reason for the choice of carbides was the desire to block, in the coating, silicon and chromium in a phase different from a solid solution, thus inhibiting their possible inward diffusion away from the surface alloy during thermal exposure.

2. Experimental procedure

The 35 NCD 16 steel (Fe–0.38 C–4 Ni–1.8 Cr–0.4 Mo, wt%) was processed by Ugine S.A., France. Its as-received hardness was 400–430 HV. Samples were cut with dimensions 12 mm × 12 mm × 2.5 mm, polished on silicon carbide papers to 1200 grit, rinsed in deionized water, then in ethanol and finally dried in hot air.

The carbide powders (Cr_3C_2 and SiC) in the diameter range of 5 μm were supplied by Goodfellow Metals Ltd, UK; they were suspended in acetone (35 vol%) and sprayed on to the steel samples. After drying, the covered samples were irradiated under an argon atmosphere by means of a continuous wave 300 W YAG laser with a spot diameter of ~ 1 mm. A constant overlapping of laser tracks of 68% was used. Two different surface alloys were processed. The first one (A) results from one irradiation of a Cr_3C_2 deposit, whereas the second one (B) necessitates two subsequent irradiations: an initial irradiation of Cr_3C_2 as in the preceding case, followed by a second one after SiC deposition. The laser parameters (power and

0022–2461

TABLE I Experimental conditions selected for processing of the surface alloys

Surface alloys	Predeposit		Laser parameters	
	Nature	Amount ($mg\,cm^{-2}$)	Power (W)	Scanning rate ($mm\,s^{-1}$)
A	Cr_3C_2	20	250	5
B	Cr_3C_2/SiC	20/5	250/175	5/5

scanning rate) and the amounts of deposits were optimized to obtain compact, adherent and crack-free surface alloys. The selected values are given in Table I. After processing, the hardness of the surface alloys was measured by Vickers indentation under a 500 gf load.

Oxidation tests were performed in a microbalance under an oxygen flux at atmospheric pressure ($5\,l\,h^{-1}$) in isothermal conditions at 850 and 950 °C. After oxidation, samples were studied by classical methods: X-ray diffraction (XRD), scanning electron microscopy (SEM) and microprobe analysis (WDS).

3. Results

3.1. Nature and microstructure of the surface alloys

The thicknesses of the surface alloys obtained were 200 μm (A) and 250 μm (B), respectively. Average concentrations were 16 wt% Cr and 2 wt% C (A) and 12 wt% Cr, 3 wt% Si and 2.5 wt% C (B). The microstructures of surface alloys A and B are identical, showing primary dendrites (γ Fe solid solution + martensite) with interdendritic eutectic material (γ Fe + martensite)–$(Fe, Cr)_7C_3$ (Figs. 1 and 2). The resulting hardnesses were 600–750 HV (A) and 650–800 HV (B), respectively. The hardness increase is probably due to the martensite formation and to the carbide precipitates.

3.2. Oxidation tests

Weight gain versus time curves presented in Fig. 3 show the good behaviour of the chromium-containing surface alloys (A) compared with the untreated material. These alloys oxidize according to a power law $(\Delta m/s)^n = kt$ where $n \sim 1.5$.

The surface alloys containing chromium and silicon (B), exhibit an excellent behaviour. They oxidize according to a very slow linear rate law, although their chromium content is less than in samples A.

The nature of the formed products was shown to be largely modified by the A and B treatments. The untreated steel oxidizes to Fe_2O_3 (haematite), Fe_3O_4 (magnetite) and FeO (wüstite). Fig. 4 shows the respective thicknesses of these three subscales forming the external part of the oxidized scale. An internal part also appears in Fig. 4. This internal part, evidently grown by inward diffusion, is constituted by chromium-containing magnetite (~ 2 at% Cr in Fe_3O_4) whereas no chromium was identified in the external part of the scale. Metallic nickel-rich nodules are also present in this part.

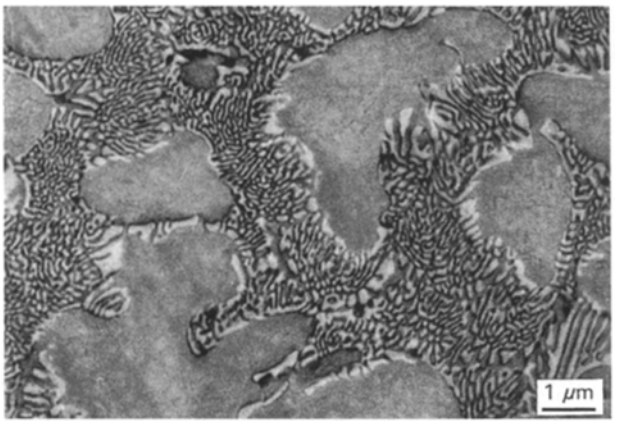

Figure 1 Scanning electron micrograph showing the different phases of 35NCD16 steel laser surface alloyed with Cr_3C_2.

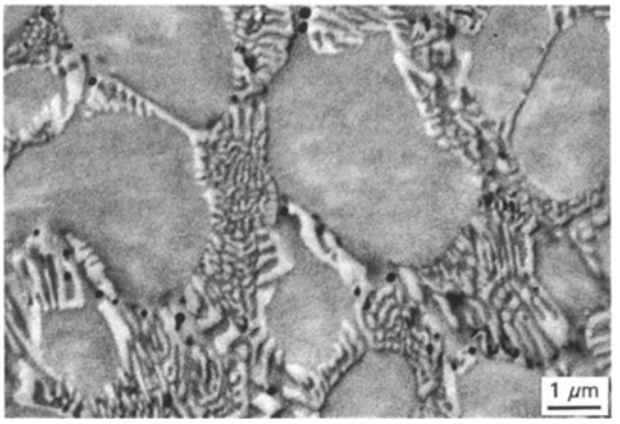

Figure 2 Scanning electron micrograph showing the different phases of 35NCD16 steel laser surface alloyed with Cr_3C_2 and SiC.

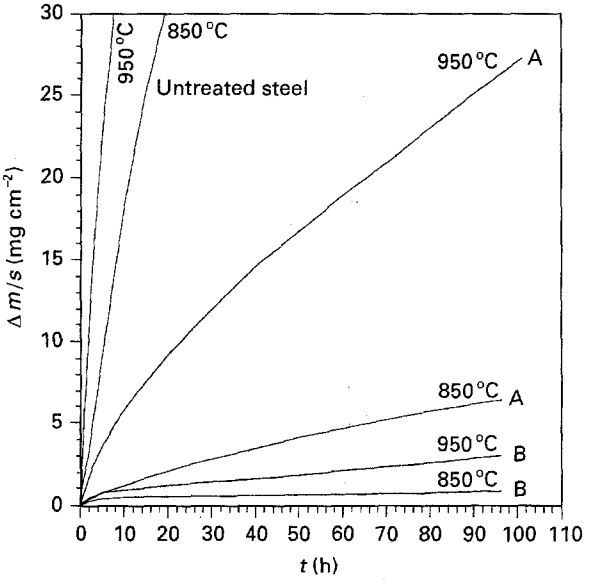

Figure 3 Weight gain versus time curves for the oxidation of 35NCD16 steel as-received and laser alloyed with Cr_3C_2 (A) or Cr_3C_2 and SiC (B).

After treatment with chromium carbide (samples A) the corrosion scale is much thinner and the X-ray mapping image exhibits three subscales (Fig. 5): an external layer of low chromium (3 at%) haematite, an

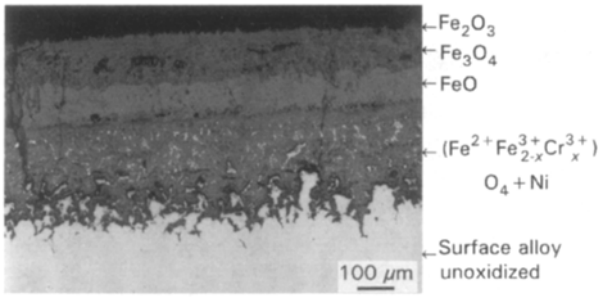

Figure 4 Cross-section of the oxidized scale formed at 850 °C after 50 h on 35NCD16 as-received steel.

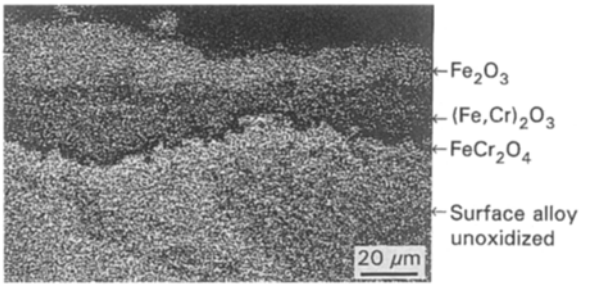

Figure 5 X-ray Fe map (WDS) on a cross-section of the oxidized scale formed at 950 °C after 96 h on the laser-treated steel 35NCD16 with Cr_3C_2.

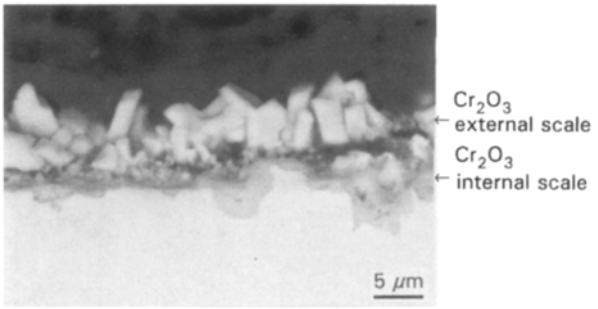

Figure 6 Cross-section of the oxidized scale formed at 950 °C after 96 h on the laser-treated steel 35NCD16 with Cr_3C_2 and SiC.

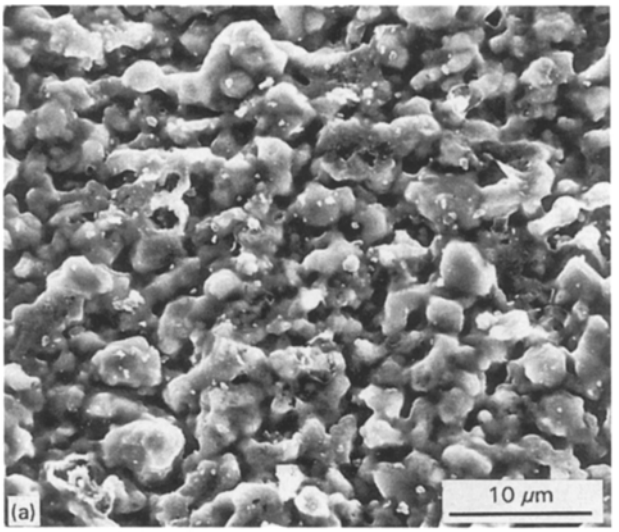

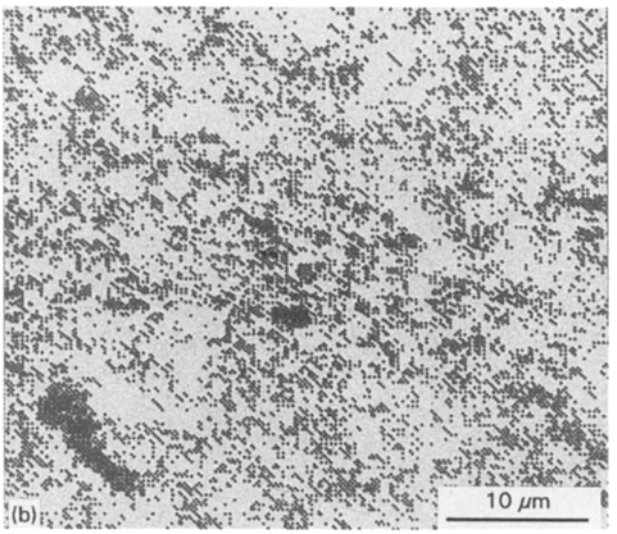

Figure 7 (a) The internal side of the removed oxide scale formed at 950 °C after 96 h on the laser-treated steel 35NCD16 with Cr_3C_2 and SiC. (b) X-ray Si map (EDS) of (a).

intermediate layer of high chromium (21 at % Cr)–haematite and a thin (5 μm) $FeCr_2O_4$ layer in contact with the treated steel. On samples B (Cr_3C_2 + SiC), the corrosion scale is very thin and was constituted of quasi-pure Cr_2O_3. Nevertheless, two subscales may be distinguished: an outer one with large crystals containing 1–2 at % iron and an inner, much more compact one, with 5 at % Fe and 0.5 at % Si (Fig. 6). Silicon enrichments were observed at the interface between these two layers after removing the external one (Fig. 7), but no crystallized silica was detected by XRD.

4. Discussion

4.1. Untreated steel

During the oxidation of the untreated steel, chromium and nickel are quasi-immobile, allowing the external growth of iron-rich oxide layers. These elements remain in the inward-growing part of the scale, in solid solution within magnetite ($Fe^{2+}Fe^{3+}_{2-x}Cr^{3+}_xO^{2-}_4$) or in the form of elementary nickel, unoxidized in this low-oxygen potential environment.

The presence of this magnetite layer under wüstite may possibly be due to the presence of dissolved chromium ions lowering the free enthalpy of formation of Fe_3O_4. Assuming a linear variation of this free enthalpy with the chromium concentration, the stability of the chromium-containing magnetite exceeds that of wüstite as soon as the chromium concentration is equal to 3.8 at %. This roughly calculated value is of the same order as that of 2 at %, measured in the internal part of the corrosion scale by microprobe analysis. Moreover, taking into account the lowering of the iron activity in the surface alloy at its interface with the oxidized scale due to iron outward diffusion, the calculated value falls and is, for example, 1.4 at % for an iron activity of 0.5.

4.2. Samples enriched with Cr_3C_2

When treated by chromium carbide (samples A) the steel is superficially enriched by chromium and,

during oxidation, the formation of an iron chromite thin layer is very effective in reducing the external iron flux. Consequently, the magnetite and the wüstite are no longer thermodynamically stable and only haematite can form.

According to Yearian *et al.* [6], who showed that the predominant defects in iron chromite are cation vacancies, it can be thought that oxygen inward diffusion is also reduced compared to what happens in the case of untreated steel, leading to the slow oxidation rate observed here.

The shape of the rate law is difficult to explain, but could result from the combination of the parallel contributions of oxygen and iron transport, with a limiting interfacial step.

4.3. Samples enriched with Cr_3C_2 and SiC

The formation of Cr_2O_3 alone, due to the lack of stability of iron oxides, results from the presence of silicon. Indeed the enrichment of this element observed at the interface between the two parts (external and internal) of the scale is probably the result of the initial rapid formation of silica, which is the most stable oxide in the system. Only Cr_2O_3 is therefore allowed to grow through grain-boundary diffusion of either chromium or oxygen, as pointed out by Beauvais–Reveillon [14]. The linear rate law observed seems not to be due to slow diffusion of chromium within a dechromized part of the surface alloy, because only a slightly dechromized layer was observed by microprobe measurements. It can be rather thought that the silicon-rich interface between the two chromia layers of the corrosion scale acts as a constant-thickness efficient barrier, inhibiting the passage of oxygen and chromium. Nevertheless, such a scale was not clearly seen especially by energy dispersive spectrometry (EDS), and this model remains partially speculative.

5. Conclusion

It was shown possible to elaborate, by laser alloying, interesting surface alloys on the 35 NCD 16 ferritic steel. A treatment with Cr_3C_2 is efficient in increasing the surface hardness and reducing the oxidation degradation by a factor of 10 at least. A still better treatment with subsequent SiC incorporation was shown to give similar or slightly higher hardness but presenting a stainless steel behaviour with the formation of Cr_2O_3 alone in oxygen at high temperature. Consequently, this treatment reduces the oxidation rates by a factor of 50 at least.

References

1. M. J. BESSLEY, "Lasers and Their Applications" (Taylor and Francis, London, 1971).
2. H. MAILLET, "Le Laser. Principes et Techniques d'Application" (Lavoisier, Paris, 1990).
3. J. F. ELOY, "Les Lasers de Puissance" (Masson, Paris, 1985).
4. S.B. NEWCOMB and W.M. STOBBS, *Mater. Sci. Technol.* **4** (1988) 384.
5. J. DECROIX, R. DAVIN and R. CASTRO, *Mém. Sci. Rev. Mét.* **60** (1963) 665.
6. H. J. YEARIAN, E. C. RANDELL and T. A. LONGO, *Corrosion* **12** (1956) 55.
7. A. U. SEYBOLT, *J. Electrochem. Soc.* **107** (1960) 147.
8. D. P. WHITTLE, G. C. WOOD, D. J. EVANS and D. B. SCULLY, *Acta Metall.* **15** (1967) 1747.
9. C. W. TUCK, *Corros. Sci.* **5** (1965) 631.
10. I. SVEDUNG and N. G. VANNERBERG, *ibid.* **14** (1974) 391.
11. H. E. EVANS, D. A. HILTON, R. A. HOLM and S. J. WEBSTER, *Oxid. Metals* **19** (1983) 1.
12. J. H. DAVIDSON, in "Ecole d'Hiver du CNRS", edited by G. Béranger, J. C. Colson and F. Dabosi (Editions de Physique, Paris, 1987) p. 395.
13. J. C. RAWERS, *Oxid. Metals* **29** (1988) 371.
14. S. BEAUVAIS-REVEILLON, PhD thesis, University of Paris Sud, Centre d'Orsay (1994).

Received 8 November 1994
and accepted 9 November 1995